Temperature Compensated Magnetostatic Wave Resonator Microsystem

Renyuan Wang[#], Connor Devitt[*], Eric Langlois[#], Sudhanshu Tiwari[*], Anuj Ashok[*], Sunil Bhave[*]
[#]BAE Systems, Inc., USA
[*]Purdue University, USA
renyuan.wang@baesystems.com, devitt@purdue.edu

***Abstract*—This work reports a compact temperature compensating permanent magnet assembly to provide static bias for micro-machined distributed magnetostatic forward volume wave (MSFVW) resonators. The cuboid-shaped assembly is 8.2 mm × 8.2 mm × 6.3 mm and provides strong static magnetic field to bias MSFVW resonators at a frequency of 19.65 GHz. Compensated by the bias assembly, the resonator exhibits a temperature coefficient of frequency (TCF) of -26.81 ppm/K compared to uncompensated TCF of $+359$ ppm/K. The temperature compensated resonator shows a quality factor of 1050 and a coupling coefficient of 4% at room temperature.**

***Keywords*— Magnetostatic forward volume wave (MSFVW), yttrium iron garnet (YIG), temperature compensation.**

I. Introduction

The microwave bands in the 3–30 GHz range are of vital interest in the defense industry. Recent advent of 5G and the desire for large bandwidth has also brought this band into prominence for commercial applications [1]. Representing the collective spin precession in ferro/ferrimagnetic solids, magnetostatic wave (MSW) resonators and filters are promising solutions for super high frequency (SHF) radios as due to their small size and high performance. Specifically, the ferrimagnetic insulator yttrium iron garnet (YIG) has demonstrated its potential as a promising platform for novel MSW applications [2] due to its low magnon damping. Devices including resonators, filters, and circulators, have been created using YIG. Conventional YIG devices are large and consist of hand-assembled multichip modules [3-5] and are biased and tuned using bulky, power-hungry electromagnets [6]. Biasing using permanent magnet assemblies is an attractive alternative for fixed frequency low power applications. However, achieving strong magnetic field for operation beyond the X-band while maintaining high temperature stability and compact form factor remains challenging [7], [8].

In this work, we match the temperature coefficients of a distributed MSFVW resonator and a compact permanent magnet bias assembly to achieve temperature compensation. We co-design a temperature compensated YIG resonator chip inside a micro-magnetic assembly and enable X-band operation with small temperature sensitivity.

II. Frequency Compensation Design

MSFVW exists in perpendicularly magnetized ferro/ferrimagnetic thin-films as a wave-vector parallel to the film. The dispersion of the lowest order mode is [9]

$$\omega^2 = \omega_0\left[\omega_0 + \omega_M\left(1 - \frac{1-e^{-kd}}{kd}\right)\right], \quad (1)$$

where $\omega_0 = \mu_0\gamma H_{eff}^{DC}$, $\omega_m = \mu_u\gamma M_s$, and ω and k are the frequency and wave-vector respectively, d is the film thickness, γ is the gyromagnetic ratio, μ_0 is the vacuum permeability, M_s is the saturation magnetization, and H_{eff}^{DC} is the effective static magnetic bias field internal to the material. For $kd \ll 1$ (thin-film approximation), the frequency tuning sensitivity is $d\omega/dH_{eff}^{DC} = (d\omega/d\omega_0)\cdot\left(d\omega_0/dH_{eff}^{DC}\right) \approx \mu_0\gamma = 2\pi \cdot 2.8$ MHz/Oe. Here, M_s exhibits strong temperature dependence, and H_{eff}^{DC} can be affected by several temperature-dependent factors including the magnetocrystalline anisotropy [10], thermal stress induced magnetoelastic effect [11], and the demagnetization field [12]. In addition, the thermal expansion of resonator body also affects the wave-vector (therefore frequency) of resonance. Among these factors, for YIG, the temperature dependence of saturation magnetization dominates resonator performance.

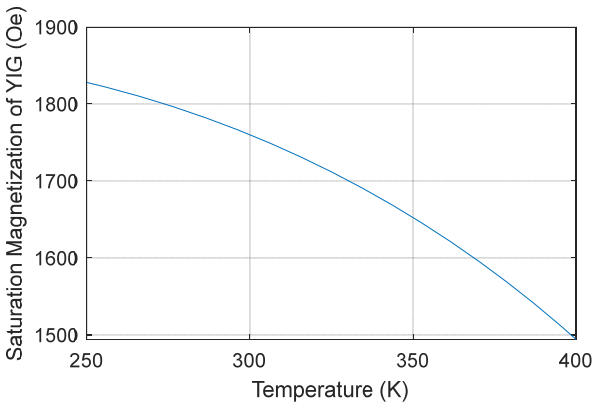

Fig. 1. Calculated saturation magnetization of YIG as a function of temperature.

The saturation magnetization below the Curie temperature and above cryogenic temperatures can be approximated by [13], [14]

$$\frac{M_s}{N\mu} = \tanh\left(\frac{M_s}{N\mu}\cdot\frac{T_C}{T}\right) \quad (2)$$

$$\mu = \gamma\mu_B/2 \quad (3)$$

where T is the temperature, T_C is the Curie temperature, N is the number of atoms per unit volume, and μ_B is the Bohr magneton. For single crystal YIG, T_C is 545 K and M_s at 300 K is 1760 Oe. Hence, M_s can be numerically calculated as shown in Fig. 1. For a perpendicularly magnetized thin film,

the internal magnetic field [15] due only to the external bias (H_{Ext}) and demagnetization field is

$$H_{eff}^{DC} = H_{Ext} - M_S. \quad (4)$$

Due to the magnetization alone, a change of temperature from 250 K to 400 K results in a frequency change of 335 Oe × 2.8 MHz/Oe = 938 MHz, or equivalently an average TCF of +347 ppm/K at a center frequency of 18 GHz.

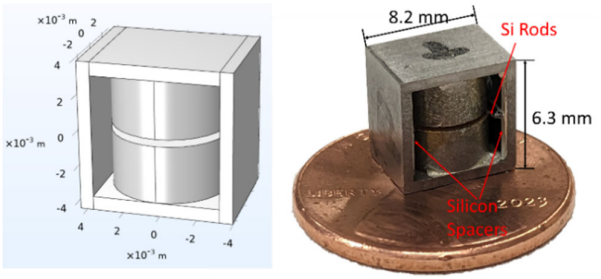

Fig. 2. 3D schematic and a photo of the temperature compensated bias assembly on a U.S. penny.

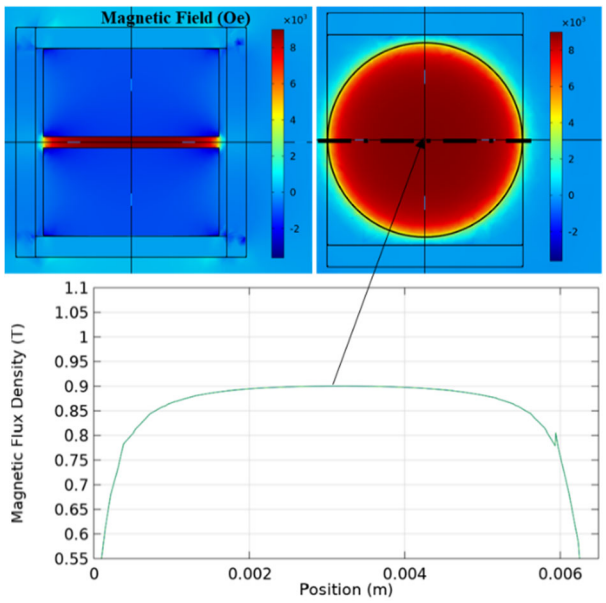

Fig. 3. Simulated performance of the micromagnetic bias assembly.

When such devices are biased using permanent magnets, the external bias from permanent magnets also decreases with increasing temperature as permanent magnets are also ferromagnetic. Therefore, by matching the temperature coefficients of the magnet and the magnetization of YIG, one can achieve temperature compensation of YIG MSFVW devices. Fig. 2 (left inset) shows a 3D schematic of the temperature compensated bias design. Two grade 26, 0.25 in. diameter, 0.125 in. thick, SmCo permanent magnets were used in the bias assembly, and the magnets' average temperature coefficient of induction is -0.035 %/K matching well with YIG near ambient. The yoke frame is designed to use Hiperco 50, of which the high saturation magnetization (2.4 T) minimizes saturation of the yoke and the total volume of the frame. Its high Curie temperature (1211 K) and weak temperature dependence of magnetic properties also minimizes the impact of TCF. The top and bottom yoke plates are 0.75 mm thick, and the yoke plates on the sides are 0.7 mm thick. The two magnets, with their north poles aligned in the same direction, contact the top and bottom yoke plates respectively, and are separated by an air gap to accommodate the resonator chip. A smaller gap will reduce the gap's magnetic reluctance, and therefore increase magnetic bias for operation beyond X-band. Our thinned and bulk micromachined chip-scale YIG resonator devices enabled us to employ a gap of only 400 μm, resulting in a simulated peak flux density of 9000 Oe (Fig. 3). This gap also allows sufficient separation between the resonator and the magnets to prevent resonator RF performance degradation due to the high loss from SmCo at microwave frequencies. The magnets are separated from the side plates by 250 μm gaps to minimize direct shorting of flux from the circumference of the magnets. Within a radius of 1.35 mm from the center axis of the magnets, the bias field is uniform within 1% which is sufficient to bias a large number of MSW devices without degrading the quality factor due to bias non-uniformity.

The entire assembly is only 8.2 mm × 8.2 mm × 6.3 mm (Fig. 2 right-inset), and the yoke frame is machined from a single piece of Hiperco 50 alloy to avoid air gaps from assembled parts. The designed assembly results in a local magnetic potential minimum, so the magnets self-assemble to the desired configuration by simply inserting the magnets into the frame. Two 250 μm thick silicon spacers are attached to the inner side surfaces of the yoke preventing the magnets from contacting the frame and shorting the magnetic flux. In addition, two 380 μm thick silicon rods are inserted at the edges of the gap between the magnets to prevent the gap from closing, since the configuration with the gap closed is another local potential energy minimum.

III. Distributed MSFVW Resonator

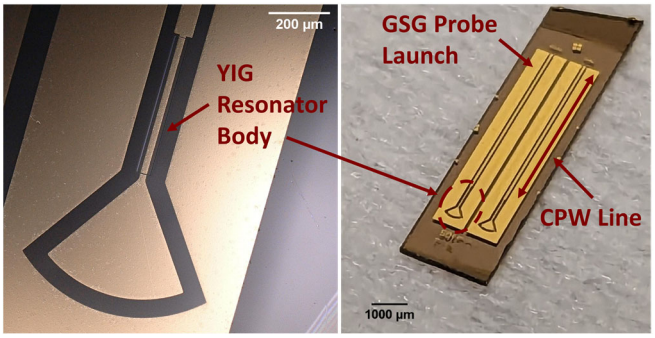

Fig. 4. Microphotograph of a distributed MSFVW resonator. The long CPW enables connection between the resonator inside the micro-magnet assembly and the RF probe outside.

The YIG resonator operates in the lowest order MSFVW mode and employs a distributed design (Fig. 4) to achieve high coupling factor [16]. To accommodate for the bias assembly, a long coplanar waveguide (CPW) transition connects the probe launch to the resonator, and the GGG substrate is thinned to 100 μm after device fabrication so that the YIG resonator is approximately positioned in the middle of the assembly gap when the bottom of the chip contacts the bottom magnet. To prevent RF loss from the bottom magnet, a

300 nm thick gold metal layer is evaporated on the backside of the thinned chip to shield the resonator.

IV. Measurements

We first measure the resonator biased using a calibrated electromagnet at room temperature to establish performance baseline (Fig. 5). 1-port s-parameters are measured using an Agilent PNA E8364B with non-magnetic GSG probes (GGB Model 40A) calibrated to the probe tip. 2-port CPW thru structures fabricated on the same substrate are used to de-embed the long CPW connection between the probe launch and the resonator (Fig. 4). An out-of-plane magnetic bias is provided by a custom electromagnet (DEXINMAG DXHD10-08) with a 10 mm pole surface diameter and two top crescent shaped yoke for improved bias uniformity. The magnetic bias is calibrated using a single-axis Gauss meter (DEXINMAG DX-150). Fig. 5 (right inset) shows the measured de-embedded impedance spectrum of a resonator with a 500 μm long, 50 μm wide YIG resonator body under a static magnetic bias of 8381 Oe. It exhibits a high quality factor of 1178 and a coupling factor [17,18] of 2.35% at a resonant frequency of 19.63 GHz.

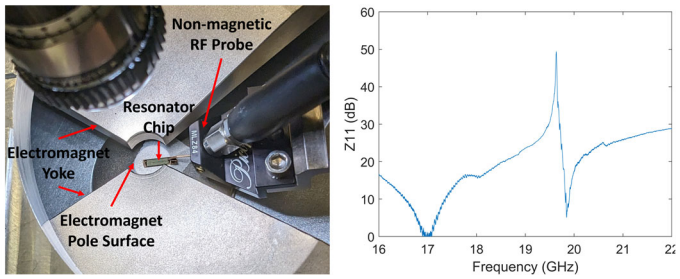

Fig. 5. Room temperature characterization setup using an electromagnet (left). Measured de-embedded resonator impedance spectrum biased at 8381 Oe using an electromagnet at room temperature (right).

The temperature stability of the compensated device was measured using the setup shown in Fig. 6. The resonator chip is held in place with vacuum on an aluminum platform to prevent magnetic interference with the bias assembly. The bias assembly is attached using silver paste to a two-stage Thorlabs TECD2 thermoelectric element powered by a Thorlabs TED4015 TEC controller. This assembly is then attached to a micro-manipulator to accurately position the resonator body at the center of the gap between the magnets while ensuring the backside of the chip makes thermal contact with the bottom magnet. Closed-loop temperature control is achieved using temperature feedback from a Thorlabs TH100PT thermistor attached to the assembly.

Fig. 7 shows the measured de-embedded impedance spectrum of the same device (measurement results in Fig. 5) for temperatures from 287 K to 335 K. The measured resonant frequency of 19.65 GHz confirmed biasing field of 8385 Oe generated by the SmCo magnets at room temperature. The resonant frequency variation as a function of temperature is summarized in Fig. 8, which shows a TCF of –0.5269 MHz/K or equivalently –26.81 ppm/K. Fig. 8 also plots the measured uncompensated TCF of the same device biased with a constant magnetic field using an electromagnet. The uncompensated TCF is +7.05 MHz/K, or equivalently +359 ppm/K, which matches well with the 347 ppm/K theoretical value. As the magnetization of YIG decreases with increasing temperature, a positive uncompensated TCF for YIG agrees with theory, and a negative compensated TCF indicates the compensation effect from the magnetic bias assembly. Temperature stability of resonator coupling factor and quality factor was also characterized (Fig. 9) with the device in the assembly. Minimal temperature dependency of coupling was observed, and the quality factor is consistently over 900 above ambient temperature thereby experimentally proving no performance degradation.

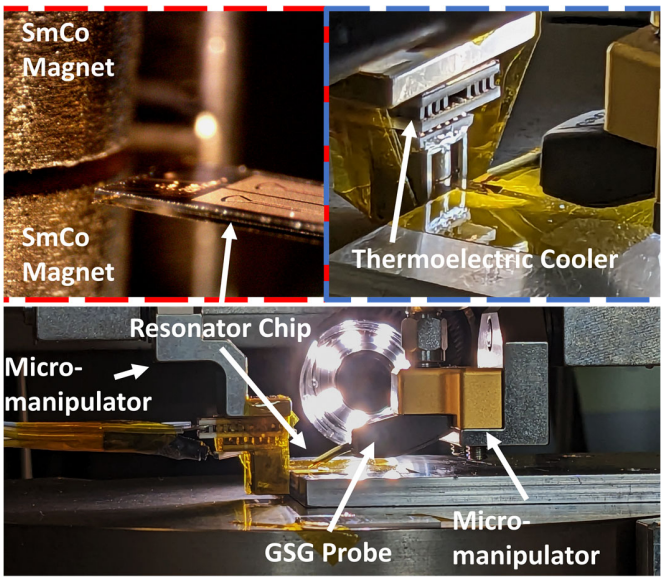

Fig. 6. Experimental setup for characterizing device temperature stability.

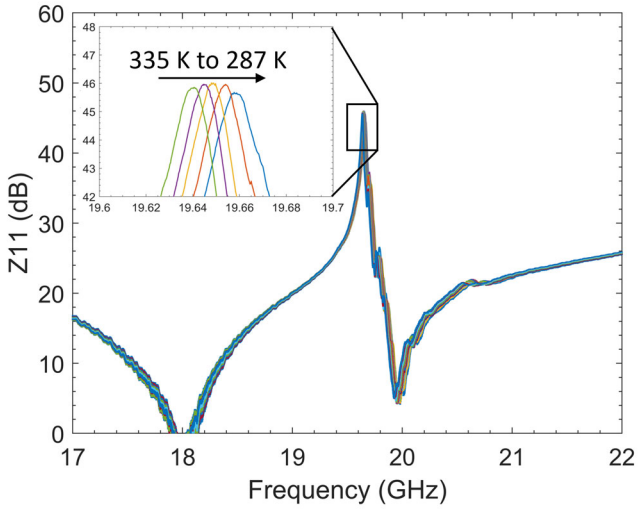

Fig. 7. Measured impedance spectrum of a 500 μm long, 50 μm wide temperature compensated MSFVW resonator device for temperatures from 287 K to 335 K

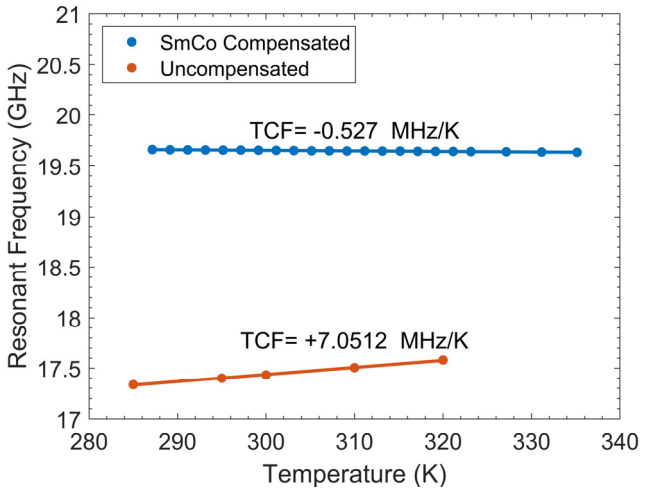

Fig. 8. Resonant frequency of the MSFVW resonator vs. temperature with and without temperature compensation.

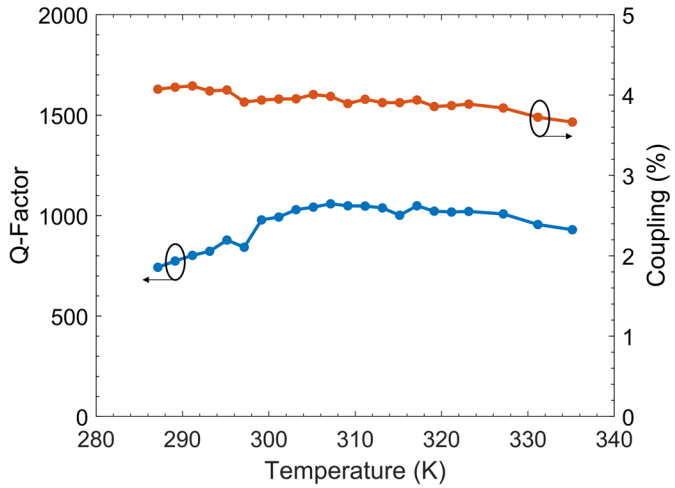

Fig. 9. Measured resonator coupling and quality factor over temperature. Resonator is biased by the temperature compensating SmCo assembly with a resonance of 19.65 GHz at 295 K.

V. Conclusion

We report a compact temperature compensating assembly to provide static bias for distributed MSFVW resonators. This results in a resonator TCF of -26.81 ppm/K without degrading the resonator performance as compared to biasing using large and power-hungry electromagnets. A 19.65 GHz resonant frequency was achieved, while the volume of the assembly is only $0.424\ \text{cm}^3$. Reducing the size by using modern fabrication and assembly techniques, and co-design of the YIG resonator with the SmCo magnetic assembly enabled temperature compensated operation.

Acknowledgment

R.W and E.L. designed and manufactured the temperature compensating micro-bias assembly. C.D. and S.T. designed the resonators. C.D., A.A., and S.T. fabricated the chip. C.D. and S.T. measured the resonators in the micro-bias assembly and performed data analysis. Manuscript was prepared by R.W. and C. D. with inputs from E.L., S.T., A.A., and S.A.B.

Chip fabrication and characterization was performed at Birck Nanotechnology Center and Seng-Liang Wang Hall at Purdue respectively. This research was developed with funding from Air Force Research Laboratory (AFRL) and the Defense Advanced Research Projects Agency (DARPA). The views, opinions and/or findings expressed are those of the authors and should not be interpreted as representing the official views or policies of the Department of Defense or the U.S. Government. This manuscript is approved for public release; distribution A: distribution unlimited.

The code and data used to produce the plots within this work will be provided upon reasonable request.

References

[1] World Radiocommunication Conference (2019). [Online]. Available: https://www.itu.int/en/ITU-R/conferences/wrc/2019/Pages/default.aspx

[2] A. A. Serga, A. V. Chumak, and B. Hillebrands, "YIG magnonics," *J. Phys. D, Appl. Phys.*, vol. 43, no. 26, Jun. 2010, doi: 10.1088/0022-3727/43/26/264002.

[3] R. Marcelli, P. De Gasperis, and L. Marescialli, "A tunable, high Q magnetostatic volume wave oscillator based on straight edge YIG resonators," *IEEE Trans. Magn.*, vol. 27, no. 6, pp. 5477–5479, Nov. 1991.

[4] S. A. Manuilov, R. Fors, S. I. Khartsev, and A. M. Grishin, "Submicron Y3Fe5O12 film magnetostatic wave band pass filters," *J. Appl. Phys.*, vol. 105, no. 3, 2009, doi: 10.1063/1.3075816.

[5] N. Zhu, X. Han, C.-L. Zou, M. Xu, and H. X. Tang, "Magnon-photon strong coupling for tunable microwave circulators," *Phys. Rev. A, Gen. Phys.*, vol. 101, no. 4, Apr. 2020.

[6] The Teledyne Defense Electronics website (2023). [Online]. Available: https://www.teledynedefenseelectronics.com/rf&microwave/products/yigproducts/Pages/YIG%20Products.aspx

[7] J. D. Adam, "A Temperature Stabilized Magnetostatic Wave Device," *Proceedings of IEEE IMS 1979*, Orlando, FL, USA, 1979, pp. 160-161, doi: 10.1109/MWSYM.1979.1124005.

[8] H. L. Glass, "Temperature Stabilization of Ferromagnetic Resonance Field in Epitaxial YIG by Ga La Substitution", *Mat. Res. Bull.*, vol. 12, pp. 735-740, 1977.

[9] D. D. Stancil, *Theory of Magnetostatic Waves*. New York, NY, USA: Springer, 2012.

[10] B. D. Cullity and C. D. Grahm, *Introduction to Magnetic Materials*, Hoboken, New Jersey, USA: John Wiley & Sons, Inc., 2009.

[11] J. Smit and H. G. Beljers, "Ferromagnetic resonance absorption in $BaFe_{12}O_{19}$, a highly anisotropic crystal," *Philips Res. Rep.*, no. 10, pp. 113-130, 1955.

[12] M. Farle, "Ferromagnetic resonance of ultrathin metallic layers," *Rep. Prog. Phys.*, no. 61, pp. 755-826, 1998.

[13] C. Kittel, *Introduction to Solid State Physics*, 8th ed., Hoboken, New Jersey, USA: John Wiley & Sons, Inc., 2005.

[14] F. J. Dyson, "General theory of spin-wave interactions," *Phys. Rev.*, no. 102, pp. 1217-1230, 1956.

[15] C. Kittel, "Ferromagnetic resonance," *J. Phys. Radium.*, no. 12, pp. 291-301, 1951.

[16] C. Devitt, S. Tiwari, S. A. Bhave, and R. Wang, "A Distributed Magnetostatic Resonator." arXiv, 2024. doi: https://doi.org/10.48550/arXiv.2401.08911.

[17] Y. Feng, S. Tiwari, S. A. Bhave and R. Wang, "Micromachined Tunable Magnetostatic Forward Volume Wave Bandstop Filter," in *IEEE Microwave and Wireless Technology Letters*, vol. 33, no. 6, pp. 807-810, June 2023, doi: 10.1109/LMWT.2023.3267449.

[18] S. Dai, S. A. Bhave, and R. Wang, "Octave-Tunable Magnetostatic Wave YIG Resonators on a Chip," *IEEE Trans. Ultrason., Ferroelect., Freq. Contr.*, vol. 67, no. 11, pp. 2454–2460, Nov. 2020, doi: 10.1109/TUFFC.2020.3000055.